Identifying a Upper-Limb Phase-Dependent Variable under Perturbations for Powered Prosthesis Arm Control

Matthew Haupmann, Mia Huang, George Selly, Leia Bagesterio, and David Quintero

***Abstract*— This paper investigates upper-limb kinematic reaching responses during a mechanical perturbation to understand interjoint arm coordination used towards powered prosthesis control development. Common prosthesis arm controllers use electromyography sensors with data-driven models to decode muscle activation signals in controlling prosthesis joint movements. However, these control approaches produce non-natural, discrete movements with no guarantee the controller can react to unexpected disturbances during continuous task motion. Determining a continuous phase-dependent variable for measuring a human's progression during reaching can derive a time-invariant kinematic function to control the prosthesis joint in a natural, continuous manner. A perturbation experimental study was conducted across three participants in evaluating the shoulder and elbow joint kinematics to examine the existence of a phase shift during reaching. Experimental results demonstrated the effects of arm proximal-distal interjoint coordination that validated the proposed mechanical phase variable of the shoulder used in parameterizing elbow joint kinematic for reaching. This could allow for a continuous phase-based control strategy that can handle disturbances to achieve arm reaching in prosthesis control.**

I. INTRODUCTION

Upper-limb amputees are more often to experience medical amputations due to a traumatic event or a systemic disease such as cancer [1]. In general, amputees will use an upper-limb prosthesis that is either 1) passive (i.e., a cosmetic limb with no active movement) or 2) body-powered (i.e., a cable tension system anchored about the upper body for manual control movement). For a body-powered prosthesis, there is an amputee rejection rate ranging between 16% to 66% due to discomfort or breakdown of the mechanical device [2]. Recently, electric-powered prostheses (e.g., myoelectric) have been more accepted with increase movement capability and provide a more intuitive feedback control of the artificial limb. Yet, there is still a relatively high rejection rate of up to 75% using such a device, mainly due to the control complexity to perform different tasks, sensory feedback reliability, and lack of training services [3], [4]. Therefore, much work is needed to develop novel control strategies to improve the versatility of advance prostheses technology for amputees [5].

A myoelectric transhumeral (above-elbow) prosthesis use electromyography (EMG) sensors to measure muscle co-contractions that is processed through complex machine learning algorithms for decoding human motion intent for control [6], [7]. However, these sensory signals require advanced signal processing with large data-driven training models to meet high classification accuracy (e.g., 85-95%) for deciphering motion intent [8]. These challenges make it difficult to provide a safe, clinically viable powered prosthesis for the vast majority of upper-limb amputee users.

Due to limitations of myoelectric prostheses, a kinematic-based control strategy can overcome these challenges to provide a robust, natural arm movement to complete daily tasks. Previous work have conducted kinematic motion planning for upper-limb prostheses by using knowledge of the coordination between interjoint limbs [9], [10]. The shoulder and elbow joints exhibit coordination with their internal dynamics to perform reaching as the hand achieves a desired target position [11]. Even so, upper-limb joint kinematic studies are observed with respect to time, while human limb movement is performed in a continuous time-invariant manner. To develop a time-invariant signal, such as a phase variable, that can measure the progression of a start to end motion task (e.g., arm reaching) can provide a phase-dependent prosthesis controller for synchronizing the joints through kinematic parameterization. A mechanical phase variable over time can either increase or decrease monotonically in measuring the current state of a motion task, and can respond to kinematic changes in phase due to external perturbations [12]. Phase-dependent control strategies using a phase variable have demonstrated stable autonomy for powered prostheses of the lower-limbs [13], [14].

An effective human motor control is the ability to counter unexpected perturbations in the environment [15]. Perturbations can be delivered at the beginning [16], after a certain period of time [17], or specific distance [18] while evaluating the arm kinematic response. Observing the biomechanical nature of human joint control under perturbation, can provide an avenue to developing control strategies for wearable robotics (e.g., powered prosthesis or exoskeletons) [19], [20]. The study entails upper-limb perturbations to understand the shoulder and elbow kinematic interaction of an occurring phase shift in defining an upper-limb phase variable.

In this paper, a phase variable about the shoulder joint is defined by observing the proximal-distal joint interaction between the shoulder and elbow joints under perturbation. Experiments were conducted with three healthy participants performing sagittal plane reaching movements with unexpected perturbations while grasping a two degree-of-freedom (DOF) end-effector perturbation machine. Participants were under randomized forward speed perturbations applied midway during reaching at predefined markers. A motion capture

M. Haupmann, G. Selly and D. Quintero are with the School of Engineering, San Francisco State University, San Francisco, CA, 94132 USA (corresponding author e-mail: qdavid@sfsu.edu). M. Huang and L. B. Bagesteiro are with the Kinesiology Department, San Francisco State University, San Francisco, CA, 94132, USA.

system recorded the upper-body joint kinematics to analyze the shoulder and elbow joint responses to observe a change in phase. The results will indicate the proposed shoulder phase variable can enforce the elbow joint progression due to the leading effect of proximal-distal joint interaction [21]. This motivates future work in determining the effectiveness of a phase-dependent variable for upper-limb prosthesis control implementation.

II. METHODS

A. Upper-Limb Phase Variable Design

The proposed upper-limb phase variable (i.e., a time-invariant signal) is related to the leading joint hypothesis for multi-joint limb movement [11]. The arm's biomechanical properties relies on high inertias and interaction torques exerted between proximal and distal joint segments. The mechanical advantage of a proximal joint (e.g., shoulder) over a distal joint (e.g., elbow) motion influences the movement progression between limbs. We aim to identify the shoulder joint angle in representing the phase-dependent variable as a bounded, monotonic signal that can parameterize the arm progression during reaching task. The phase variable algorithm is derived as a normalized function between 0 and 1 signifying the start and end points of completing the progression of reaching, respectively. This was similarly presented as a declared phase variable for lower-limb of utilizing the thigh angle as the proximal joint that had a mechanical influence for multiple distal joints with regards to the knee and ankle joints during gait [22], [23]. The phase variable is normalized by scaling the global shoulder angle (i.e., angle measured about the vertical gravity vector) by

$$\phi_s = \frac{\theta_s - \theta_s^{min}}{\theta_s^{max} - \theta_s^{min}}, \tag{1}$$

where θ_s is the measured shoulder angle, θ_s^{min} is the minimum shoulder angle, and θ_s^{max} is the maximum shoulder angle. The shoulder minimum and maximum angles are constant values represented by the start and end points of the arm reaching progression, respectively, when the arm begins colinear with the global vertical gravity vector along the sagittal plane. These values can be adjusted per participant's comfort level from start to finish of their reaching task. The normalized phase variable ϕ_s will produce an increasing value from the shoulder's angle continuous change during reaching. The phase variable can be parameterized to a desired elbow actuated joint trajectory function for prosthesis feedback control design.

B. Experimental Setup & Protocol

1) Experimental Hardware: A multi-DOF robot (Genmark, GPR-GB8-SM) was the perturbation machine that interacted between the participants (see Fig. 1). The robot has 8 motorized axes with two-link paddle arms as dual independent end-effectors with each providing fast translatory motion. Only one end-effector arm link was used allowing 0.50 m of capable unidirectional linear travel for perturbation motion. A custom 3D printed joystick (0.095 m in height, 0.051 m sphere diameter on top) with an adapter aluminum plate mounted to the end-effector for grasping onto the perturbation machine. Prior to experiments, we tested the robot's end-effector transient response time at a 0.10 m linear travel step input producing a rise time of 0.11 ms, which is greater than the minimum perturbation time at 10 ms to have no significance in change of kinematics [24]. The global up/down z-axis end-effector location can be adjusted per a participant's height for comfortable arm resting position in having the shoulder angle roughly at 0 degrees and elbow flexed at 90 degrees. When the perturbation machine is unpowered, the end-effector connecting joint is direct motor control with low friction and inertia to allow smooth motion travel during reaching. The desired joint command profiles and feedback measurements were passed through the robot controller's RS232 serial communication port using MATLAB R2019b (Mathworks Inc., Natick, MA). Six Vicon MX13 motion capture cameras (Oxford Metrics Ltd., Oxford, UK) paired with Vicon Nexus software (v2.10) were used to capture the upper-body joint movements from reflective markers 3D coordinates at a 100 Hz sample rate.

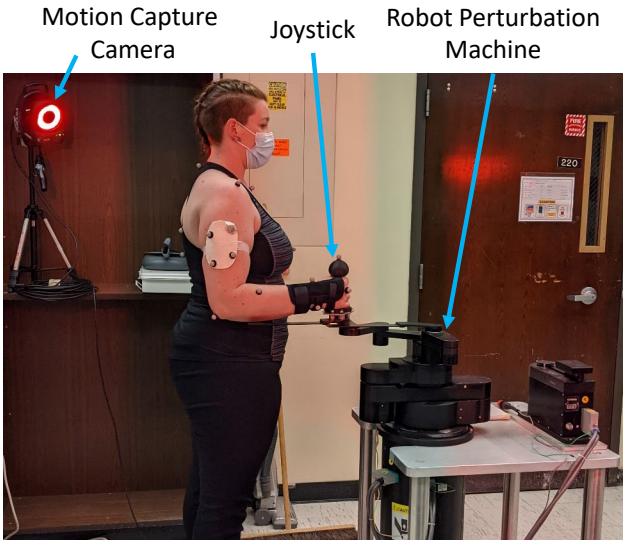

Fig. 1. Able-bodied participant grasping robot perturbation machine at the end-effector with an attached custom joystick. The participant performs forward arm reaching along the sagittal plane while wearing a rigid wrist brace to restrict out-of-plane motion. A motion capture system with reflective markers placed along the participant's upper-body and the perturbation machine to track kinematic motion in 3D space.

2) Experimental Procedure: The experimental protocol was reviewed and approved by the Institutional Review Board (IRB) at San Francisco State University. Experiments were conducted by three able-bodied participants (1 male, 2 females; averages: age = 27.3 years, height = 1.74 m, mass = 83.2 kg). Reflective markers were placed on participants upper body following Vicon's upper body musculoskeletal model. Participant's wore a size-adjustable rigid wrist brace to limit wrist motion, so the study may focus on shoulder and elbow joint kinematics along the sagittal plane. All reaching trials were performed with the right arm.

Participants were instructed to grasp the joystick at a comfortable distance from the robots x-y zero position. Their right arm was placed along the side of their trunk with the elbow flexed at $\sim$90 degrees and shoulder at $\sim$0 degrees about their standing vertical axis (see Fig. 1). Participants were then instructed to push the joystick forward at their comfortable reaching speed in an upright position without moving their trunk or correcting for the perturbation until the arm was fully extended. Participants were given an acclimation period to move the joystick freely in the forward translation motion. Subsequently, they performed 45 trials of forward reaching while grasping the perturbation joystick.

Trials were randomized to perform a third (i.e., 15 trials) of each perturbation condition: normal speed, fast speed, and non-perturbed with two marker locations. Participants had no knowledge of the occurrence of perturbation prior to movement. A perturbation marker consists of a specific location during forward travel motion, where the robot holds the joint positions static for a brief moment (i.e., time of 40 ms the robot receives and processes a command) before it continues moving forward. Perturbation studies use marker locations as a conventional approach to create a datum of when a perturbation or non-perturbation may occur in a reaching motion [25], [26]. Each trial included two different marker locations. The first perturbation marker (Marker 1) occurred a forward distance of 0.076 m from the participant's starting rest position. The second marker (Marker 2) location was set at a distance of 0.10 m from Marker 1, a total of 0.18 m from the starting rest position. The participant is able to complete the full arm reaching extension beyond Marker 2. Thus, the marker locations were chosen to be within the participants' full travel distance for reaching. Between markers, the randomized trials were either a non-perturbation (robot unpowered and end-effector can move freely) or a speed perturbation (robot powered and end-effector has a programmed set speed) trial. The two perturbation linear speeds were set at 1.02 m/s and 1.52 m/s for a normal and fast speed, respectively. At both speeds, the robot constant acceleration was set at 0.64 m/s^2. In all, the reaching sequence consisted of participants reaching forward freely until Marker 1, then either a non-perturbation or speed perturbation occurred until Marker 2, and then after can move freely without restriction to complete arm extension. A completed trial was when participants reached full arm extension and moved the joystick back to its initial (zero) position (i.e., participants resting position with the elbow at 90 degrees). Upon return to the robot's zero position, the participants will feel the robot lock indicating end of the trial. Afterwards, participants were free to let go of the joystick and continue to the next trial run.

III. RESULTS & DISCUSSION

Participants were instructed to begin voluntarily at their comfortable start time to perform a forward reaching trial. The analyzed results start time (e.g., t=0 sec) began once the robot detected positive forward motion (linear velocity $>$ 0 m/s) as a participant is extending their arm forward while grasping the joystick. Figure 2 shows the shoulder and elbow joint angles mean and $\pm$1 standard deviation for all three participants across the different perturbation trials. Once Marker 1 (vertical grey dash line) is reached, all three participants experienced a kinematic phase shift for both shoulder and elbow joints during normal and fast speed perturbation compared to the non-perturbation (baseline) trials. Observing Subject 1 results, the shoulder angle begins to have a phase shift at t=0.76 secs and the joint angle does not continue along its trajectory path until reaching t=0.85 secs causing a Δt=0.09 secs time shift. About t=1.09 secs, Marker 2 is reached causing another phase shift before the normal and fast perturbations kinematics reaches the final steady-state values near the non-perturbation kinematics. The normal perturbation produced the longest duration time at 2.7 secs to reach full arm extension, while the fast perturbation had the largest angle difference of 8 degrees compared to the non-perturbation trials. Both Subjects 2 and 3 produce similar phase shift occurrences between the non-perturbation versus speed perturbations. However, they both produced a slightly longer end time duration for shoulder and elbow for the fast perturbation compared to the normal perturbation. Subject 3 had a larger variance compared to Subjects 1 and 2 for the different trials. This may be caused by having a higher payload applied to the robot end-effector as Subject 3 weighed about 5 kgs more and had the largest overall right arm length compared to the other participants. Increasing the velocity perturbation depending on participant size may reduce variance and mitigate overpower resistance to the forces induced by the perturbation machine. In all, a phase shift is evaluated across the participants between non-perturbation and the speed perturbations (both normal and fast). For the speed perturbations, a deceleration occurred before it recovers to its kinematic trajectory path towards the end of arm extension. This caused a phase shift in reaching task completion as non-perturbation reaches final mean shoulder and elbow joint angle earlier compared to the speed perturbations. Between perturbation speeds, the normal speed completes final mean shoulder and elbow joint angle for reaching sooner than the fast speed perturbation with the exception of Subject 1. The perturbation results demonstrating the phase shift by the joint deceleration of task completion provides a relationship for defined phase variable from the shoulder angle to determining the kinematic progression of the elbow.

Fig. 3 displays the upper-limb normalized phase variable over time derived from Eq. 1 using mean shoulder angle from Subject 1. A phase shift is further demonstrated, and the non-perturbation versus speed perturbations converge towards the tail-end of the reaching task (phase variable=0.975). The phase variable increases over time with the exception when Marker 1 (t=0.475sec) and Marker 2 (t=1.09sec) occurred, where the signal was no longer increasing but decreasing. This decrease was due to a hardware limitation encountered when the robot powered on/off cycle at each marker caused the robot to stop instantly, which caused the shoulder and elbow joints to decelerate and reverse in the opposite di-

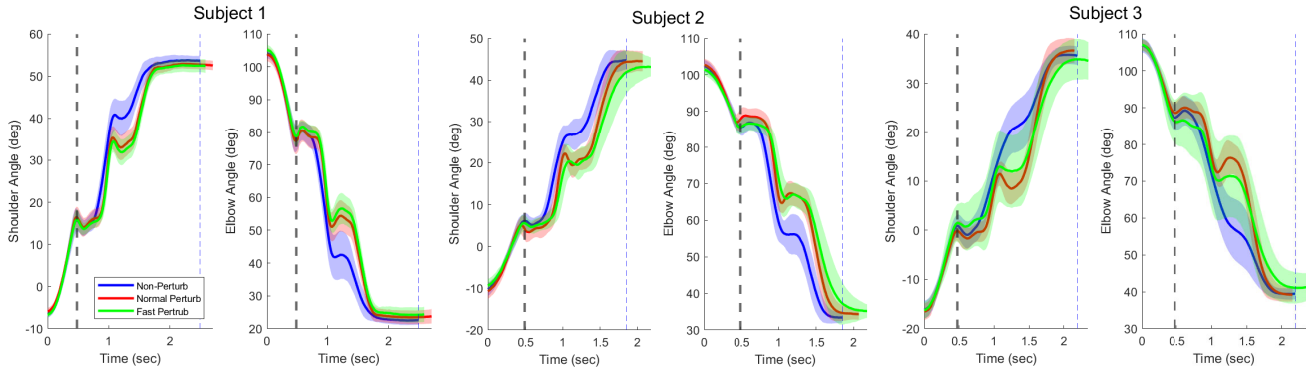

Fig. 2. The shoulder and elbow joint angles versus time for the three perturbation categories: non-perturbation (Non-Perturb, blue solid line), normal speed perturbation (Normal Perturb, red solid line), and fast speed perturbation (Fast Perturb, green solid line). The solid lines indicates the mean joint angles across each of the 15 trials per perturbation category and their respective shaded region of ± 1 standard deviation. The vertical thick grey dash line indicates Marker 1 location of when a perturbation was initialized. The vertical thin dash blue line is the end time for when full extension is achieved for the non-perturb mean travel.

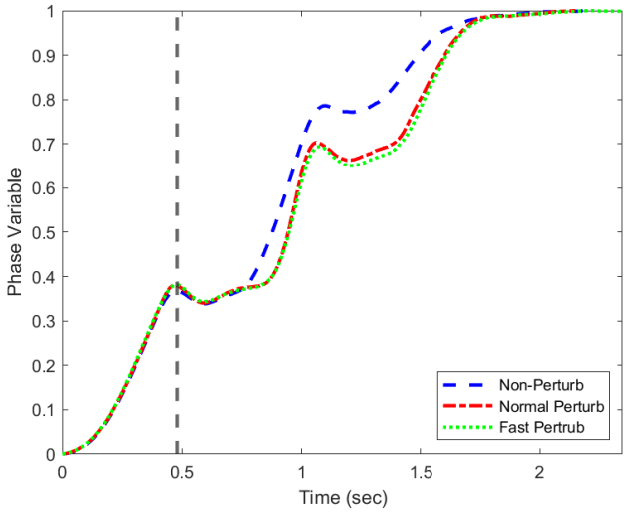

Fig. 3. Subject 1 normalized phase variable versus time at different perturbation trials. Non-perturbation (Non-Perturb, blue dashed line), normal speed perturbation (Normal Perturb, red dash-dot line), and fast speed perturbation (Fast Perturb, green dotted line) each displays an increasing signal with the exception when a marker location is reached (e.g., Marker 1 (grey dash line)).

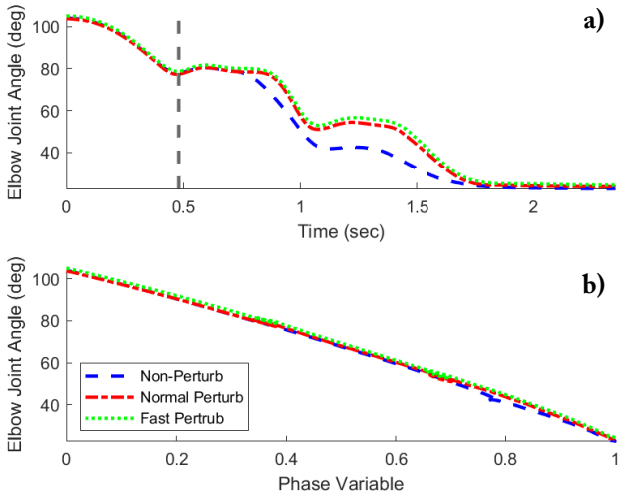

Fig. 4. Subject 1 mean elbow joint angles versus time a) and versus normalized phase variable b) for the different perturbation trials. For a), Marker 1 is indicated by the vertical thick grey dash line, which produced a phase shift until the normal and fast perturbation returned to the non-perturbation trial. For b), the speed perturbations converge to the non-perturbation response when elbow joint angle is evaluated against the phase variable.

rection before continuing through arm extension. However, it had no effect of receiving the phase shift from occurring once Marker 1 location was met.

Final results of the kinematic relationship of the mean elbow joint angle versus time (Fig. 4a)) and parameterized against the phase variable (Fig. 4b)) for Subject 1. Comparing the parameterization of the elbow joint angle versus time or phase variable produces a different curvature when referring to the time-domain or phase-domain, respectively. Elbow joint angle versus phase variable for the different perturbation trials are merged as a linearly decreasing response demonstrating that in phase-domain the elbow kinematics is speed-invariant. This analysis can be extended to perform higher speed perturbations to understand the effects speed change has in a phase-based control strategy.

IV. CONCLUSION

We proposed a phase-dependent variable based on the proximal shoulder joint angle to determine the continuous progression of the distal elbow joint during reaching. Perturbation experiments evaluated the existence of a phase shift during reaching while perturbed. Different speed perturbation trials were evaluated across three participants with each having a clear phase shift to the shoulder and elbow joint kinematics, demonstrating an extended completion time for reaching compared to non-perturbation trials. The experiments validated the theory of proximal-distal joint interaction dynamics with the shoulder enforcing the elbow kinematic behavior. A phase variable was derived from the shoulder joint producing an increase signal during progression of arm reaching. Future work is to parameterize a desired elbow

kinematic trajectory function for reaching based on the proposed phase variable for prosthesis control. Current efforts are to build a prosthesis elbow control testbed to implement this phase-based control strategy to perform amputee subjects experiments.

V. ACKNOWLEDGMENT

The authors thank Joey Menicucci for designing and manufacturing the 3D printed joystick attached to the perturbation machine.

REFERENCES

[1] S. J. Cuccurullo, *Physical medicine and rehabilitation board review*. Springer Publishing Company, 2019.

[2] E. A. Biddiss and T. T. Chau, "Upper limb prosthesis use and abandonment: a survey of the last 25 years," *Prosthetics and orthotics international*, vol. 31, no. 3, pp. 236–257, 2007.

[3] R. C. Crandall and W. Tomhave, "Pediatric unilateral below-elbow amputees: retrospective analysis of 34 patients given multiple prosthetic options," *Journal of Pediatric Orthopaedics*, vol. 22, no. 3, pp. 380–383, 2002.

[4] D. Silcox 3rd, M. D. Rooks, R. R. Vogel, and L. L. Fleming, "Myoelectric prostheses. a long-term follow-up and a study of the use of alternate prostheses." *The Journal of bone and joint surgery. American volume*, vol. 75, no. 12, pp. 1781–1789, 1993.

[5] C. Lake and J. M. Miguelez, "Comparative analysis of microprocessors in upper limb prosthetics," *JPO: Journal of Prosthetics and Orthotics*, vol. 15, no. 2, pp. 48–63, 2003.

[6] Y. Huang, K. B. Englehart, B. Hudgins, and A. D. Chan, "A gaussian mixture model based classification scheme for myoelectric control of powered upper limb prostheses," *IEEE Transactions on Biomedical Engineering*, vol. 52, no. 11, pp. 1801–1811, 2005.

[7] R. N. Khushaba, A. H. Al-Timemy, A. Al-Ani, and A. Al-Jumaily, "A framework of temporal-spatial descriptors-based feature extraction for improved myoelectric pattern recognition," *IEEE Transactions on Neural Systems and Rehabilitation Engineering*, vol. 25, no. 10, pp. 1821–1831, 2017.

[8] N. Parajuli, N. Sreenivasan, P. Bifulco, M. Cesarelli, S. Savino, V. Niola, D. Esposito, T. J. Hamilton, G. R. Naik, U. Gunawardana, *et al.*, "Real-time emg based pattern recognition control for hand prostheses: a review on existing methods, challenges and future implementation," *Sensors*, vol. 19, no. 20, p. 4596, 2019.

[9] F. Lacquaniti and J. F. Soechting, "Coordination of arm and wrist motion during a reaching task," *Journal of Neuroscience*, vol. 2, no. 4, pp. 399–408, 1982.

[10] Y. Losier, K. Englehart, and B. Hudgins, "Evaluation of shoulder complex motion-based input strategies for endpoint prosthetic-limb control using dual-task paradigm." *Journal of Rehabilitation Research & Development*, vol. 48, no. 6, 2011.

[11] N. Dounskaia, "The internal model and the leading joint hypothesis: implications for control of multi-joint movements," *Experimental Brain Research*, vol. 166, no. 1, pp. 1–16, 2005.

[12] D. J. Villarreal, D. Quintero, and R. D. Gregg, "A perturbation mechanism for investigations of phase variables in human locomotion," in *2015 IEEE International Conference on Robotics and Biomimetics (ROBIO)*. IEEE, 2015, pp. 2065–2071.

[13] R. D. Gregg, T. Lenzi, L. J. Hargrove, and J. W. Sensinger, "Virtual constraint control of a powered prosthetic leg: From simulation to experiments with transfemoral amputees," *IEEE Trans. Robot.*, vol. 30, no. 6, pp. 1455–1471, 2014.

[14] D. Quintero, D. J. Villarreal, D. J. Lambert, S. Kapp, and R. D. Gregg, "Continuous-phase control of a powered knee–ankle prosthesis: Amputee experiments across speeds and inclines," *IEEE Trans. Robot.*, vol. 34, no. 3, pp. 686–701, 2018.

[15] I. L. Kurtzer, J. A. Pruszynski, and S. H. Scott, "Long-latency reflexes of the human arm reflect an internal model of limb dynamics," *Current Biology*, vol. 18, no. 6, pp. 449–453, 2008.

[16] G. Koshland and Z. Hasan, "Electromyographic responses to a mechanical perturbation applied during impending arm movements in different directions: one-joint and two-joint conditions," *Experimental brain research*, vol. 132, no. 4, pp. 485–499, 2000.

[17] J. E. Schaffer and R. L. Sainburg, "Interlimb responses to perturbations of bilateral movements are asymmetric," *Journal of motor behavior*, vol. 53, no. 2, pp. 217–233, 2021.

[18] C. R. Lowrey, J. Y. Nashed, and S. H. Scott, "Rapid and flexible whole body postural responses are evoked from perturbations to the upper limb during goal-directed reaching," *Journal of neurophysiology*, vol. 117, no. 3, pp. 1070–1083, 2017.

[19] R. D. Gregg, E. J. Rouse, L. J. Hargrove, and J. W. Sensinger, "Evidence for a time-invariant phase variable in human ankle control," *PLoS ONE*, vol. 9, no. 2, p. e89163, 2014.

[20] D. J. Villarreal, D. Quintero, and R. D. Gregg, "A perturbation mechanism for investigations of phase-dependent behavior in human locomotion," *IEEE Access*, vol. 4, pp. 893–904, 2016.

[21] N. Dounskaia, "Control of human limb movements: the leading joint hypothesis and its practical applications," *Exercise and sport sciences reviews*, vol. 38, no. 4, p. 201, 2010.

[22] D. J. Villarreal, D. Quintero, and R. D. Gregg, "Piecewise and unified phase variables in the control of a powered prosthetic leg," in *2017 International Conference on Rehabilitation Robotics (ICORR)*. IEEE, 2017, pp. 1425–1430.

[23] D. Quintero, D. J. Villarreal, and R. D. Gregg, "Preliminary experiments with a unified controller for a powered knee-ankle prosthetic leg across walking speeds," in *2016 IEEE/RSJ International Conference on Intelligent Robots and Systems (IROS)*. IEEE, 2016, pp. 5427–5433.

[24] T. Cluff and S. H. Scott, "Rapid feedback responses correlate with reach adaptation and properties of novel upper limb loads," *Journal of Neuroscience*, vol. 33, no. 40, pp. 15 903–15 914, 2013.

[25] S. H. Brown and J. D. Cooke, "Responses to force perturbations preceding voluntary human arm movements," *Brain Research*, vol. 220, no. 2, pp. 350–355, 1981.

[26] C. R. Lowrey, J. Y. Nashed, and S. H. Scott, "Rapid and flexible whole body postural responses are evoked from perturbations to the upper limb during goal-directed reaching," *Journal of neurophysiology*, vol. 117, no. 3, pp. 1070–1083, 2017.